

Adaptive DNN Partitioning and Offloading in Heterogeneous Edge-Cloud Continuum

Akuen Akoi Deng^{*[0009-0007-6228-3340]}, Eimantas Butkus^{*[0009-0001-5647-0779]},
Alfreds Lapkovskis^[0009-0003-4424-949X], and
Praveen Kumar Donta^[0000-0002-8233-6071]

Department of Computer and Systems Sciences, Stockholm University,
Borgarfjordsgatan 12, Stockholm, Sweden
{akuiendng, butkus505}@gmail.com
{alfreds.lapkovskis, praveen}@dsv.su.se

Abstract. In recent years, the use of artificial intelligence on resource-constrained IoT devices has grown significantly. However, existing approaches to DNN partitioning and offloading across the edge-cloud continuum typically rely on static methods that ignore runtime dynamics. Furthermore, they are often evaluated in simulated environments rather than on real hardware. To address this gap, we propose a framework that dynamically splits neural network layers across the heterogeneous continuum. The framework profiles the model at startup, measures network link conditions between nodes, and periodically re-evaluates the partition to adapt to environmental changes. We created a physical testbed comprising a Raspberry Pi edge device, a laptop fog, and a high-performance desktop PC as the cloud. We evaluated the framework over three widely adopted convolutional neural networks: VGG16, AlexNet, and MobileNetV2. Our results show that the framework achieves reductions in energy and end-to-end latency of 27.09–35.82% and 6.34–22.92%, respectively, compared to a static partitioning baseline. These findings confirm the superiority of adaptive to static partitioning.

Keywords: Model Partitioning · Edge Computing · Distributed Inference · Computing Continuum · Internet of Things · Task Offloading

1 Introduction

In recent years, the widespread adoption of Internet-of-Things (IoT) devices has led to unprecedented growth in the volume, velocity, and variety of data generated [1, 6, 15]. These devices range from smartphones and wearables to RFID readers and tablets, increasingly supporting applications with strict requirements for latency, energy efficiency, and computational workload [1, 14], such as smart homes, robotics, virtual reality, autonomous driving, and M2M communications [9, 15]. Simultaneously, rapid advancements in artificial intelligence (AI), specifically deep neural networks (DNNs), have enabled fast and sophisticated data-driven decision-making across diverse fields [3, 18].

* These authors contributed equally to this work.

Traditionally, AI models have been deployed and executed in a centralized environment, such as the cloud, which provides abundant computational resources. However, this approach introduces significant limitations when applied to IoT systems [1]. In an IoT environment, network latency, privacy concerns, bandwidth constraints, and poor connectivity can significantly degrade real-time system performance [2]. This has driven the research toward a computing continuum spanning cloud, edge, fog, and IoT devices [5], where computing is increasingly distributed across these heterogeneous tiers to meet the demands of modern AI applications [19]. This approach allows some parts of the AI workload to run on edge devices alongside the central cloud servers, a model known as edge-cloud AI, promising to combine the low-latency benefits of edge computing with the scalability of the cloud [15, 20, 22].

However, designing adaptive and efficient AI systems for resource-constrained edge devices remains challenging due to the inherent heterogeneity of the edge-cloud environment, where devices vary widely in computational capability, energy budget, and network conditions [4, 16]. To address this, researchers have explored distributed training, deployment, and inference of AI models across heterogeneous nodes [4, 10, 12].

In distributed inference, AI workloads are split across edge and cloud devices, allowing latency-critical tasks to execute close to the data source while more computationally intensive operations are offloaded to the cloud [23, 24]. However, most current approaches rely on static deployment with predefined inference pipelines that do not adapt to runtime changes. Factors such as fluctuating bandwidth, workload contention, and node mobility make fixed partitioning decisions inefficient in dynamic environments [1], frequently resulting in performance degradation. This motivates the need for an adaptive partitioning and offloading framework that dynamically distributes AI workloads across edge-cloud resources while satisfying stringent latency and energy constraints.

The literature on adaptive DNN partitioning and offloading in heterogeneous edge-cloud networks has expanded significantly in recent years [1, 11, 17]. Proposed approaches include reinforcement learning-based layer partitioning strategies [17, 21], collaborative caching mechanisms [7], and edge-end joint parallel inference architectures [23]. However, a key limitation of many existing solutions is their reliance on simulated environments that assume ideal network conditions [11, 13, 21], leaving the practical performance of these methods in real-world deployments insufficiently explored.

Li et al. [11] proposed a framework that jointly optimises fine-grained DNN layer partitioning and magnitude-based channel pruning to reduce inference latency, using an LSTM-based controller trained with a policy gradient algorithm and a delay-aware reward function. Despite promising results, the evaluation was conducted entirely through simulation in an MEC environment.

Studies conducted in real environments, e.g., [7], tend to focus on metrics such as task completion time, while overlooking energy consumption and computational load balancing. Fang et al. [8] proposed EdgeDI, which compresses models via structured pruning and a lightweight attention-based convolutional

block, then partitions feature-map workloads across industrial IoT devices using an execution-time-aware scheme that accounts for both computation capability and network bandwidth. While EdgeDI achieves notable inference speedups, the work focuses exclusively on inference performance, leaving energy consumption unaddressed.

These examples reflect a consistent trend in the literature: partitioning and offloading frameworks are predominantly evaluated in simulation, and energy consumption is rarely a primary design objective in heterogeneous edge-cloud environments.

This work addresses both gaps through real-world experimentation on resource-constrained hardware, proposing an adaptive partitioning and offloading framework that minimizes energy consumption without violating real-time latency constraints. Our contributions are threefold:

- We propose an adaptive partitioning and offloading framework for DNN inference across a heterogeneous edge-cloud continuum.
- We build a fully functional three-tier testbed comprising a Raspberry Pi edge device, a laptop fog node, and a high-performance PC cloud node, enabling evaluation of vertical offloading strategies on real hardware.
- We conduct real-world experiments over three widely adopted convolutional neural network (CNN) models (VGG16, AlexNet, and MobileNetV2), collecting and evaluating hardware-measured energy and latency metrics across single-device, static partitioning, and adaptive partitioning configurations.

The remainder of this paper is organized as follows. Section 2 presents the proposed adaptive partitioning framework. Section 3 describes the experimental setup and discusses the results. Section 4 concludes the paper.

2 Proposed Framework

We assume a continuum environment with an edge, fog, and a cloud node. In this architecture, inference is initiated on the edge device, intermediate DNN activations are deployed to the fog, and the remaining computations are performed on the cloud. This allows partitioning schemas with $0, \dots, i$ layers on the edge, $i + 1, \dots, j$ layers on the fog, and $j + 1, \dots, N - 1$ layers on the cloud, where $1 \leq i < j < N$ are layer indices.

The proposed framework dynamically partitions and offloads CNN inference workloads across nodes to minimize energy consumption without exceeding latency limits. At runtime, the framework periodically evaluates the current partition against available resources. It only reconfigures the workload if real-time computation and communication measurements predict a more optimal split.

The framework follows a five-stage algorithmic pipeline: (i) offline profiling, (ii) two-point link probing, (iii) candidate split estimation, (iv) best candidate search, and (v) adaptive distributed inference scheduling. The following sections detail these stages.

2.1 Offline Profiling

The offline profiler runs once before any partitioning decision is made, producing two lookup tables used throughout the framework. The first is an activation size table, which records the size of the intermediate tensor in bytes at every feature boundary. For a candidate split (i, j) , this gives the number of bytes the Raspberry Pi must transmit to the laptop after layer i , and the laptop must transmit to the PC after layer j . The second is a relative compute weight table, where each layer is assigned a normalized fraction of the total inference work based on a single measured execution. These weights serve as a stable reference that allows runtime measurements from a small number of probe splits to be scaled and generalized to estimate the latency and energy of any unseen partition. The offline profiling algorithm is shown in Algorithm 1.

Algorithm 1 Offline profiling of a neural network \mathcal{N}

Require: Pretrained network \mathcal{N} with ordered feature children $\mathcal{F} = (f_0, f_1, \dots, f_{N-1})$ and classifier head H

Ensure: Per-layer activation sizes B and relative compute weights W

```

1:  $x \leftarrow \text{randn}(1, 3, 224, 224)$ 
2: for  $k \leftarrow 1$  to 3 do ▷ warmup
3:    $x' \leftarrow H(\mathcal{F}(x))$ 
4: end for
5:  $x \leftarrow \text{randn}(1, 3, 224, 224)$ 
6: for  $i \leftarrow 0$  to  $N - 1$  do
7:    $t_0 \leftarrow \text{now}()$ 
8:    $x \leftarrow f_i(x)$ 
9:    $T[i] \leftarrow \text{now}() - t_0$ 
10:   $B[i] \leftarrow \text{numel}(x) \cdot \text{elementSize}(x)$ 
11: end for
12:  $t_0 \leftarrow \text{now}(); \_ \leftarrow H(x); T[N] \leftarrow \text{now}() - t_0$ 
13:  $W[k] \leftarrow T[k] / \sum_j T[j]$  for all  $k \in \{0, \dots, N\}$ 
14: return  $B, W$ 

```

2.2 Two-Point Link Probing

With activation sizes known, the framework must also estimate the communication cost between nodes. The two-point link probe achieves this by transmitting two payloads of contrasting sizes s_1 and s_2 across each hop, repeating each transmission multiple times and averaging the round-trip times to reduce short-term timing noise. The round-trip time for a payload of size s on hop h is modeled as

$$rtt_h(s) = \omega + \frac{s}{\beta}, \quad (1)$$

where ω is the fixed communication overhead and β is the effective throughput in bytes per second. Given the averaged round-trip times $\tau[s_1]$ and $\tau[s_2]$, the

throughput is estimated as

$$\beta = \frac{s_2 - s_1}{\tau[s_2] - \tau[s_1]} \quad (2)$$

and the fixed overhead as

$$\omega = \max\left(0, \tau[s_1] - \frac{s_1}{\beta}\right). \quad (3)$$

The resulting pair (ω, β) provides a concrete link model that the framework uses to predict the transfer time of any activation tensor at a given split point, as formalised in Algorithm 2.

Algorithm 2 Two-point link probe

Require: Hop h with round-trip function $\text{rtt}_h(s)$; sizes $s_1 \ll s_2$; repeat count r
Ensure: Link model (ω, β) where ω is fixed overhead and β is throughput in bytes/second

- 1: **for** $s \in \{s_1, s_2\}$ **do**
- 2: $\tau[s] \leftarrow \text{mean}(\{\text{rtt}_h(s) : k = 1, \dots, r\})$
- 3: **end for**
- 4: **if** $\tau[s_2] \leq \tau[s_1]$ **then return** previous model \triangleright malformed probe; keep stale values
- 5: **end if**
- 6: compute β using Eq.(2)
- 7: $\omega \leftarrow \max(0, \tau[s_1] - s_1/\beta)$
- 8: **return** (ω, β)

2.3 Candidate Split Latency and Energy Estimation

For a candidate split (i, j) , where i is the index of the last feature layer executed on the edge node and j is the last feature layer on the fog node, the estimator predicts end-to-end latency and energy consumption before the split is actually run. Latency is computed as the sum of three per-node computation times and two inter-node transfer times, derived from the profiled compute weights, the per-node execution rates, and the fitted link models. Energy is estimated per node by multiplying each node’s compute time by its corresponding power or energy rate, where the edge node applies a fixed power model, and the fog and cloud nodes use empirical rates fitted from previous runs. The total system energy is the sum of all three contributions. Since these are estimates rather than measurements, any discrepancy between the predicted and observed values is used to refine the per-node rates in the next re-evaluation cycle, as formalized in Algorithm 3.

Algorithm 3 Estimate latency and energy of a candidate split (i, j)

Require: Candidate (i, j) ; per-layer compute weights W ; per-node speeds $(\sigma_{\text{Pi}}, \sigma_{\text{Lap}}, \sigma_{\text{PC}})$; per-node energy rates $(\rho_{\text{Lap}}, \rho_{\text{PC}})$; link models $(\omega_{pl}, \beta_{pl})$ and $(\omega_{lp}, \beta_{lp})$; payload table B

- 1: $w_{\text{Pi}} \leftarrow \sum_{k=0}^i W[k]$
- 2: $w_{\text{Lap}} \leftarrow \sum_{k=i+1}^j W[k]$
- 3: $w_{\text{PC}} \leftarrow \sum_{k=j+1}^N W[k]$
- 4: $t_{\text{Pi}} \leftarrow \sigma_{\text{Pi}} \cdot w_{\text{Pi}}$; $t_{\text{Lap}} \leftarrow \sigma_{\text{Lap}} \cdot w_{\text{Lap}}$; $t_{\text{PC}} \leftarrow \sigma_{\text{PC}} \cdot w_{\text{PC}}$
- 5: $t_{pl} \leftarrow \omega_{pl} + B[i]/\beta_{pl}$
- 6: $t_{lp} \leftarrow \omega_{lp} + B[j]/\beta_{lp}$
- 7: $\hat{L} \leftarrow t_{\text{Pi}} + t_{\text{Lap}} + t_{\text{PC}} + t_{pl} + t_{lp}$
- 8: $\hat{E}_{\text{Pi}} \leftarrow P_{\text{Pi}} \cdot t_{\text{Pi}}$ $\triangleright P_{\text{Pi}}$: fixed Pi power model (12 W)
- 9: $\hat{E}_{\text{Lap}} \leftarrow \rho_{\text{Lap}} \cdot t_{\text{Lap}}$; $\hat{E}_{\text{PC}} \leftarrow \rho_{\text{PC}} \cdot t_{\text{PC}}$
- 10: $\hat{E}_{\text{tot}} \leftarrow \hat{E}_{\text{Pi}} + \hat{E}_{\text{Lap}} + \hat{E}_{\text{PC}}$
- 11: **return** $(\hat{L}, \hat{E}_{\text{Pi}}, \hat{E}_{\text{tot}})$

2.4 Best Candidate Split Search

The candidate search evaluates every valid split pair (i, j) , where validity requires each node to execute at least one layer, and returns the candidate that minimizes the objective score. For each candidate, the estimator is called to obtain the predicted latency and energies, after which two filters are applied. The first rejects any candidate whose predicted latency exceeds the deadline L_{max} , and the second rejects candidates whose normalized score exceeds that of the static baseline, guaranteeing the adaptive framework never produces a result worse than the baseline it is intended to improve upon. Candidates that pass both filters are scored using the weighted sum

$$S(i, j) \triangleq w_{\text{end}} \frac{\hat{E}_{\text{end}}(i, j)}{n_{\text{end}}} + w_{\text{tot}} \frac{\hat{E}_{\text{tot}}(i, j)}{n_{\text{tot}}} + w_{\text{lat}} \frac{\hat{L}(i, j)}{n_{\text{lat}}}, \quad (4)$$

where w_{end} , w_{tot} , and w_{lat} are user-defined weights, and the normalization anchors n are average values measured from probe splits run at startup. Here, $\hat{E}_{\text{end}}(i, j)$ and $\hat{E}_{\text{tot}}(i, j)$ denote the predicted edge node and total system energy respectively, and $\hat{L}(i, j)$ denotes the predicted end-to-end latency for split (i, j) , as estimated by Algorithm 3. Normalization makes the score dimensionless and ensures each weight exerts a comparable influence regardless of the absolute magnitude of the underlying quantities, as formalized in Algorithm 4.

2.5 Adaptive Distributed Inference Scheduling

The adaptive scheduler orchestrates the full runtime loop across two phases, with initialization handled in phase 1 and steady-state operation in phase 2.

In phase 1a, the scheduler runs a user-defined initial split for a fixed number of inferences to record the nodes' latency and energy consumption, establishing the baseline threshold that subsequent candidates must improve upon. In phase

Algorithm 4 Find best candidate split

Require: Rates and link models (as in Alg. 3); weights $\mathbf{w} = (w_{\text{Pi}}, w_{\text{tot}}, w_{\text{lat}})$; normalization anchors $\mathbf{n} = (n_{\text{Pi}}, n_{\text{tot}}, n_{\text{lat}})$; baseline score S^* ; deadline L_{max} ; minimum Pi layers m ; current split c

- 1: $(s_{\text{best}}^*, S_{\text{best}}) \leftarrow (\text{NONE}, +\infty)$
- 2: **for** $(i, j) \in \{(i, j) : m-1 \leq i < j < N\}$ **do**
- 3: **if** $(i, j) = c$ **then continue** ▷ exclude currently-running split
- 4: **end if**
- 5: $(\hat{L}, \hat{E}_{\text{Pi}}, \hat{E}_{\text{tot}}) \leftarrow \text{ESTIMATE}(i, j, \dots)$ ▷ Alg. 3
- 6: **if** $L_{\text{max}} > 0$ **and** $\hat{L} > L_{\text{max}}$ **then continue** ▷ deadline pre-filter
- 7: **end if**
- 8: $S \leftarrow w_{\text{Pi}} \cdot \frac{\hat{E}_{\text{Pi}}}{n_{\text{Pi}}} + w_{\text{tot}} \cdot \frac{\hat{E}_{\text{tot}}}{n_{\text{tot}}} + w_{\text{lat}} \cdot \frac{\hat{L}}{n_{\text{lat}}}$
- 9: **if** $S > S^*$ **then continue** ▷ must beat static baseline
- 10: **end if**
- 11: **if** $S < S_{\text{best}}$ **then**
- 12: $(s_{\text{best}}^*, S_{\text{best}}) \leftarrow ((i, j), S)$
- 13: **end if**
- 14: **end for**
- 15: **return** s_{best}^*

1b, three additional probe splits are run automatically, selected to expose edge-heavy, balanced, and cloud-heavy workload distributions, giving the estimator sufficient data to infer per-node execution rates across a wide operating range. In phase 1c, the collected baseline and probe measurements are used to fit the per-node compute rates, probe both network links, and select the best starting split by evaluating all candidates against the objective score defined in Eq. (4). Energy terms are weighted more heavily than latency, with the edge node energy weight ranging from 0.6 to 0.9, total system energy from 0.2 to 0.3, and latency from 0.1 to 0.3, reflecting the framework’s primary objective of reducing energy consumption without violating latency constraints.

In phase 2, the scheduler enters steady-state operation and runs the current split for R_{steady} inferences per window. At the end of each window, it refits the per-node compute rates using both the phase 1 data and the most recent window combined, re-probes both network links, and re-runs the candidate search with the updated parameters. A switch is made if the new candidate improves the objective score by at least 3%. If the latency deadline L_{max} is violated during a window, the switch is forced regardless of the improvement margin; if no better candidate exists under a deadline violation, the scheduler falls back to the static baseline c_0 as the safest known configuration. This periodic re-evaluation is what makes the framework adaptive, as changes in network bandwidth or node compute load are captured by the re-probing and re-fitting steps and reflected in the next candidate selection, as formalized in Algorithms 5 and 6.

Algorithm 5 Adaptive distributed inference scheduler – Initialization

Require: Model \mathcal{N} ; initial split c_0 ; weights \mathbf{w} ; deadline L_{\max} ; R_{profile} baseline runs; R_{probe} runs per probe split; R_{steady} runs per re-evaluation window; warmup k_{warm} ; switch improvement threshold θ

Phase 1a: baseline run (defines threshold to beat)

- 1: $(B, W) \leftarrow \text{PROFILE}(\mathcal{N})$ ▷ Alg. 1
- 2: $\mathcal{D}_{\text{base}} \leftarrow \emptyset$; $c \leftarrow c_0$
- 3: **for** $r \leftarrow 1$ to R_{profile} **do**
- 4: $s \leftarrow \text{RUNINFERENCE}(c)$
- 5: **if** $r > k_{\text{warm}}$ **then** $\mathcal{D}_{\text{base}} \leftarrow \mathcal{D}_{\text{base}} \cup \{s\}$
- 6: **end if**
- 7: **end for**
- 8: $(b_{\text{Pi}}, b_{\text{tot}}, b_{\text{lat}}) \leftarrow$ mean energies and latency over $\mathcal{D}_{\text{base}}$
- Phase 1b:** probe reference splits to ground per-layer rates
- 9: $\mathcal{P} \leftarrow \text{PROBESPLITS}(N, m)$ ▷ 3 splits at fifths of the feature range
- 10: $\mathcal{D}_{\text{probe}} \leftarrow \emptyset$
- 11: **for all** $p \in \mathcal{P} \setminus \{c_0\}$ **do**
- 12: **for** $r \leftarrow 1$ to R_{probe} **do**
- 13: $s \leftarrow \text{RUNINFERENCE}(p)$
- 14: **if** $r > k_{\text{warm}}$ **then** $\mathcal{D}_{\text{probe}} \leftarrow \mathcal{D}_{\text{probe}} \cup \{s\}$
- 15: **end if**
- 16: **end for**
- 17: **end for**
- Phase 1c:** fit rates, probe links, choose starting split
- 18: $\mathbf{n} \leftarrow$ mean energies and latency over $\mathcal{D}_{\text{probe}}$ ▷ normalization independent of c_0
- 19: $S^* \leftarrow w_{\text{Pi}}(b_{\text{Pi}}/n_{\text{Pi}}) + w_{\text{tot}}(b_{\text{tot}}/n_{\text{tot}}) + w_{\text{lat}}(b_{\text{lat}}/n_{\text{lat}})$
- 20: $\sigma, \rho \leftarrow \text{FITRATES}(\mathcal{D}_{\text{base}} \cup \mathcal{D}_{\text{probe}}, W)$
- 21: $(\omega_{pl}, \beta_{pl}), (\omega_{lp}, \beta_{lp}) \leftarrow \text{LINKPROBE}()$ ▷ Alg. 2
- 22: $c \leftarrow \text{FINDBEST}(\sigma, \rho, \omega, \beta, \mathbf{w}, \mathbf{n}, S^*, L_{\max}, m, \text{NONE})$ ▷ Alg. 4

3 Results and Discussion

This section presents the quantitative evaluation of the proposed adaptive partitioning framework against single-device and static partitioning baselines across three CNN models.

3.1 Experimental Setup

Experiments were conducted on a three-tier heterogeneous testbed representing a typical IoT edge-cloud hierarchy. The edge device is a Raspberry Pi 4 (4-core Arm Cortex-A76, 2.4 GHz, 8 GB LPDDR4X), representing a resource-constrained IoT node. The fog node is a laptop (Intel Core i7-10510U, 16 GB DDR4), and the cloud node is a desktop PC equipped with an NVIDIA RTX 4070 Ti GPU (7680 CUDA cores, 40.09 FP32 TFLOPS, 32 GB DDR5, 12 GB VRAM GDDR6). Nodes were interconnected via Tailscale VPN with ZeroMQ handling inter-node messaging. Network constraints and bottlenecks were simulated using Tailscale’s traffic throttling capabilities.

Algorithm 6 Adaptive distributed inference scheduler – Steady state

Require: Current split c ; baseline split c_0 ; weights \mathbf{w} ; deadline L_{\max} ; R_{steady} runs per re-evaluation window; warmup k_{warm} ; switch improvement threshold θ ;
Phase-1 data $\mathcal{D}_{\text{phase1}} = \mathcal{D}_{\text{base}} \cup \mathcal{D}_{\text{probe}}$
Phase 2: steady state with periodic re-evaluation

- 1: **while** budget not exhausted **do**
- 2: $\mathcal{W} \leftarrow \emptyset$
- 3: **for** $r \leftarrow 1$ to R_{steady} **do**
- 4: $s \leftarrow \text{RUNINFERENCE}(c)$
- 5: **if** $r > k_{\text{warm}}$ **then** $\mathcal{W} \leftarrow \mathcal{W} \cup \{s\}$
- 6: **end if**
- 7: **end for**
- 8: $\bar{L} \leftarrow \text{mean latency over } \mathcal{W}$
- 9: $\sigma, \rho \leftarrow \text{FITRATES}(\mathcal{D}_{\text{phase1}} \cup \mathcal{W}, W)$ \triangleright Phase-1 data keeps rates grounded
- 10: $(\omega, \beta) \leftarrow \text{LINKPROBE}()$
- 11: $c' \leftarrow \text{FINDBEST}(\sigma, \rho, \omega, \beta, \mathbf{w}, \mathbf{n}, S^*, L_{\max}, m, c)$
- 12: $S_c, S_{c'} \leftarrow \text{SCORE}(c, \dots), \text{SCORE}(c', \dots)$
- 13: $\Delta \leftarrow (S_c - S_{c'})/S_c$ \triangleright relative improvement
- 14: deadlineHit $\leftarrow (L_{\max} > 0 \wedge \bar{L} > L_{\max})$
- 15: **if** deadlineHit $\wedge c' \neq c$ **then**
- 16: $c \leftarrow c'$ \triangleright FORCED switch (deadline violation)
- 17: **else if** $c' \neq c \wedge \Delta \geq \theta$ **then**
- 18: $c \leftarrow c'$ \triangleright NORMAL switch
- 19: **else if** deadlineHit $\wedge c \neq c_0$ **then**
- 20: $c \leftarrow c_0$ \triangleright fall back to static baseline
- 21: **end if**
- 22: **end while**

Three widely benchmarked CNN models were evaluated: VGG16 (138M parameters, 528 MB), AlexNet (61M parameters, 234 MB), and MobileNetV2 (2.2M parameters, 8.8 MB), spanning a broad range of complexity. To isolate computational workload from dataset variability, randomly generated dummy tensors of shape $1 \times 3 \times 224 \times 224$ matching each model’s input dimensions were used as inference inputs. Models were implemented in PyTorch.

Energy consumption was measured independently per node: the edge node applied a constant 12 W power model multiplied by measured compute time, the fog node read package energy deltas via Intel RAPL through the Linux powercap interface, and the cloud node integrated instantaneous GPU power readings from NVIDIA NVML over the compute window. Latency was recorded using wall-clock timing. Two primary metrics are reported: total end-to-end inference latency (ms) and total energy consumption (J) across all active nodes.

Each configuration was executed over 500 inference passes, repeated ten times and averaged to ensure measurement stability. We compare three execution strategies: (i) single-device baseline on each node independently, (ii) static partitioning with a fixed split, approximating equal workload thirds across the

three nodes, and (iii) the proposed adaptive partitioning algorithm, which dynamically determines split points based on runtime conditions.

The implementation is publicly available on GitHub.¹

3.2 Single-Device Baselines

Table 1 reports the average per-inference latency and energy consumption for each model running entirely on a single device, with no network transfers or offloading.

Table 1. Average per-inference latency and energy consumption for single-device execution.

Device	Model	Latency (ms)	Energy (J)
Edge	VGG16	666.870	8.002
	AlexNet	132.400	1.589
	MobileNetV2	71.900	0.863
Fog	VGG16	169.908	2.549
	AlexNet	20.988	0.315
	MobileNetV2	15.954	0.239
Cloud	VGG16	1.164	0.037
	AlexNet	0.830	0.024
	MobileNetV2	4.175	0.092

Across all three models, the edge and cloud nodes differ by roughly two orders of magnitude in both latency and energy. The cloud node completes VGG16 in 1.16 ms and AlexNet in 0.83 ms, while the edge node requires 666.87 ms and 132.40 ms respectively, a gap of approximately $570\times$. MobileNetV2 shows a considerably smaller gap of $17\times$ (71.90 ms vs 4.18 ms), reflecting its design for resource-constrained inference. The fog node sits between the two extremes, with latencies of 169.91 ms, 20.99 ms, and 15.95 ms for VGG16, AlexNet, and MobileNetV2, respectively. The same ordering holds for energy: the edge node consumes 0.86–8.00 J per inference, the fog node 0.24–2.55 J, and the cloud node 0.009–0.037 J. These single-device figures exclude any network transfer cost and therefore represent idealized lower bounds rather than realistic end-to-end performance. In practice, routing all inference to the cloud introduces network latency and bandwidth constraints that make full offloading impractical in real IoT deployments, which is precisely the motivation for adaptive partitioning.

3.3 Static Partitioning Baseline

Table 2 reports the per-inference results when the three models are executed across the three-node continuum using a fixed partitioning scheme, with cut

¹ <https://anonymous.4open.science/r/EdgeCloudAIPartitioning-0E80>

points chosen to distribute roughly one-third of the feature extraction work to each node. For VGG16, this corresponds to layers 0–10 on the edge node, layers 11–30 on the fog node, and the classifier head on the cloud node. For AlexNet, layers 0–9 run on the edge node, layers 10–12 together with the adaptive average pooling module on the fog node, and the classifier on the cloud node. For MobileNetV2, the first 10 blocks run on the edge node, the remaining 9 blocks on the fog node, and the pooling and classifier head on the cloud node.

Table 2. Per-inference latency and energy consumption under static partitioning.

Model	Pipeline	Edge	Fog	Cloud	Total
	Latency (ms)	Energy (J)	Energy (J)	Energy (J)	Energy (J)
VGG16	525.142	2.297	2.491	0.905	5.693
AlexNet	78.148	0.237	0.082	0.356	0.675
MobileNetV2	98.457	0.624	0.268	0.027	0.919

Relative to the single-device baseline, static partitioning reduces end-to-end latency for VGG16 by 21.2% (from 666.87 ms to 525.14 ms) and for AlexNet by 41.0% (from 132.40 ms to 78.15 ms). MobileNetV2 behaves differently: the network transfer overhead outweighs the computational benefit, increasing end-to-end latency by 36.9% from 71.90 ms to 98.46 ms. In terms of energy, the total system cost is 5.69 J for VGG16, 0.68 J for AlexNet, and 0.92 J for MobileNetV2. The per-node energy distribution differs markedly across models: for VGG16, the load is spread relatively evenly across all three nodes (2.30 J, 2.49 J, and 0.91 J for edge, fog, and cloud, respectively), while for AlexNet and MobileNetV2 the edge node remains the dominant consumer (0.24 J and 0.62 J), with the fog node contributing considerably less (0.08 J and 0.27 J).

3.4 Adaptive Partitioning

Table 3 reports the same per-inference metrics when the adaptive scheduler controls the split points. The scheduler initializes by running 50 inferences at the static split to establish the baseline threshold, followed by 15 inferences at each of three automatically selected probe splits. It then fits the per-node compute rates and link bandwidth parameters, selects the best starting split, and enters steady-state operation with re-evaluation every 100 inferences.

Under adaptive partitioning, the total system energy is 3.65 J, 0.43 J, and 0.67 J for VGG16, AlexNet, and MobileNetV2 respectively, with end-to-end latencies of 491.86 ms, 60.23 ms, and 84.48 ms. For all three models, the adaptive framework reduces both energy consumption and latency relative to the static baseline. The per-node energy distribution shifts noticeably between the two configurations: for VGG16, the edge and fog node contributions drop from 2.30 J to

Table 3. Average per-inference latency and energy consumption under adaptive partitioning.

Model	Pipeline	Edge	Fog	Cloud	Total
	Latency (ms)	Energy (J)	Energy (J)	Energy (J)	Energy (J)
VGG16	491.855	1.489	1.235	0.930	3.654
AlexNet	60.233	0.078	0.097	0.259	0.434
MobileNetV2	84.479	0.494	0.078	0.099	0.670

1.49 J and from 2.49 J to 1.24 J respectively. For AlexNet, the edge node contribution drops from 0.24 J to 0.08 J. For MobileNetV2, the edge node drops from 0.62 J to 0.49 J, while the cloud node rises from 0.03 J to 0.10 J, reflecting a shift of heavier computation toward the more energy-efficient cloud node.

3.5 Comparison of Static and Adaptive Partitioning

Table 4 summarizes the improvements achieved by the adaptive framework over the static baseline in terms of percentage reductions in latency and total system energy.

Table 4. Reduction in latency and energy achieved by adaptive over static partitioning.

Model	Latency Reduction (%)	Energy Reduction (%)
VGG16	6.34	35.82
AlexNet	22.92	35.70
MobileNetV2	14.20	27.09

The energy reduction ranges from 27.09% for MobileNetV2 to 35.82% for VGG16, and the latency reduction ranges from 6.34% for VGG16 to 22.92% for AlexNet. Across all three models, the energy reduction consistently exceeds the latency reduction, reflecting the framework’s objective weighting. Figures 1 and 2 show the absolute latency and energy values side by side for both configurations, and Fig. 3 shows the relative reductions as percentages.

The three models differ in how the savings are distributed between energy and latency. VGG16 achieves the largest absolute and relative energy reduction (2.04 J, 35.82%) but the smallest latency reduction (33.28 ms, 6.34%), suggesting the scheduler prioritized offloading computation away from the energy-hungry edge node over minimizing transfer overhead. AlexNet achieves both a large energy reduction (0.24 J, 35.70%) and the largest latency reduction of the three models (17.92 ms, 22.92%). MobileNetV2 shows the smallest energy reduction (27.09%) alongside a moderate latency improvement of 14.20%. Across all three models, energy reductions consistently exceed latency reductions in percentage

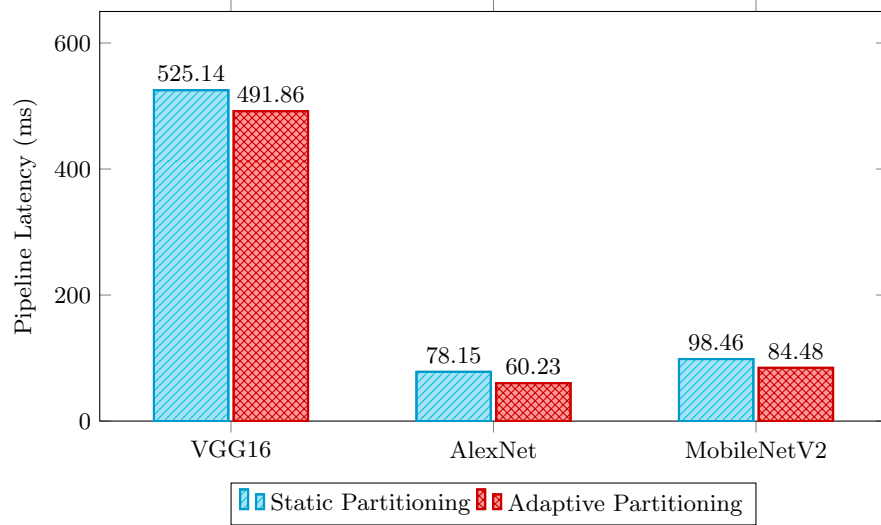


Fig. 1. Pipeline latency under static and adaptive partitioning.

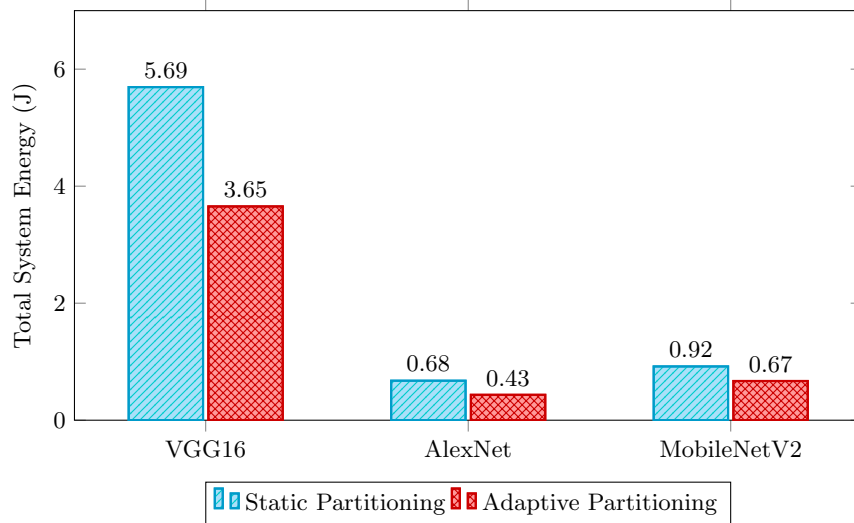


Fig. 2. Total system energy under static and adaptive partitioning.

terms, consistent with the higher weights assigned to energy terms in the objective function.

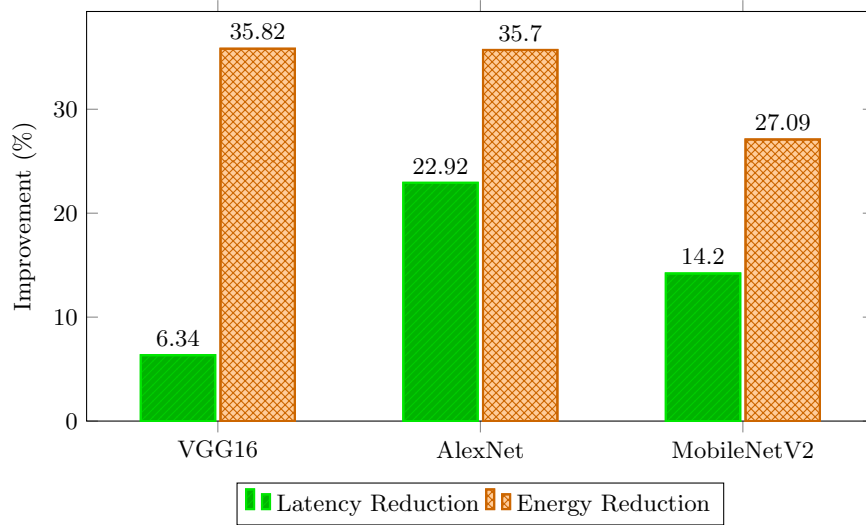


Fig. 3. Reduction in latency and energy achieved by adaptive over static partitioning.

4 Conclusions

This paper presented an adaptive partitioning and offloading framework for distributed DNN inference across a heterogeneous edge-cloud continuum, motivated by the lack of real-hardware evaluation and limited focus on energy consumption in existing works. The framework was validated on a physical testbed comprising a Raspberry Pi edge node, a laptop fog node, and a GPU-equipped cloud node, across three CNN models spanning a broad complexity range. Results show energy reductions of up to 35.82% for VGG16 and AlexNet, and 27.09% for MobileNetV2, alongside latency reductions of up to 22.92%, all relative to a static partitioning baseline. These findings confirm that adaptive partitioning can significantly reduce energy consumption on resource-constrained devices without violating latency constraints, addressing a gap that simulation-based approaches have largely been overlooked.

These results compare favorably with recent related work despite differences in optimisation objective: Li et al. [11] achieved 27.31% latency reduction through joint partitioning and pruning, Chen et al. [2] reported 34.72%–43.52% latency improvements with EdgeCI, and Fang et al. [7] demonstrated substantial power efficiency gains via DRL-based offloading. Our framework achieves comparable improvements while targeting energy consumption over latency, and unlike RL-based or parallel inference approaches, relies on a single weighted objective function evaluated periodically at runtime, making it lightweight and continuously adaptive.

References

- [1] Chen, H., Qin, W., Wang, L.: Task partitioning and offloading in iot cloud-edge collaborative computing framework: a survey. *Journal of Cloud Computing* **11**(1), 86 (2022)
- [2] Chen, Y., Luo, T., Fang, W., Xiong, N.N.: Edgeci: Distributed workload assignment and model partitioning for cnn inference on edge clusters. *ACM Transactions on Internet Technology* **24**(2), 1–24 (2024)
- [3] Dargan, S., Kumar, M., Ayyagari, M.R., Kumar, G.: A survey of deep learning and its applications: A new paradigm to machine learning. *Archives of computational methods in engineering* **27**(4) (2020)
- [4] Doan, H.N.T., Nguyen, P.N.T., Bui, B.C., Phan, N.D.: Optimizing edge device routing in edge computing: Harnessing the synergy of distributed processing and correlation analysis. In: *Proceedings of the 2024 13th International Conference on Software and Computer Applications*. pp. 368–372 (2024)
- [5] Donta, P.K., Murturi, I., Casamayor Pujol, V., Sedlak, B., Dustdar, S.: Exploring the potential of distributed computing continuum systems. *Computers* **12**(10) (2023). <https://doi.org/10.3390/computers12100198>, <https://www.mdpi.com/2073-431X/12/10/198>
- [6] Edquist, H., Goodridge, P., Haskel, J.: The internet of things and economic growth in a panel of countries. *Economics of Innovation and New Technology* **30**(3), 262–283 (2021)
- [7] Fang, C., Meng, X., Hu, Z., Xu, F., Zeng, D., Dong, M., Ni, W.: Ai-driven energy-efficient content task offloading in cloud-edge-end cooperation networks. *IEEE Open Journal of the Computer Society* **3**, 162–171 (2022)
- [8] Fang, W., Xu, W., Yu, C., Xiong, N.N.: Joint architecture design and workload partitioning for dnn inference on industrial iot clusters. *ACM Trans. Internet Technol.* **23**(1) (Feb 2023). <https://doi.org/10.1145/3551638>, <https://doi-org.ezp.sub.su.se/10.1145/3551638>
- [9] Feng, C., Han, P., Zhang, X., Yang, B., Liu, Y., Guo, L.: Computation offloading in mobile edge computing networks: A survey. *Journal of network and computer applications* **202**, 103366 (2022)
- [10] Langer, M., He, Z., Rahayu, W., Xue, Y.: Distributed training of deep learning models: A taxonomic perspective. *IEEE Transactions on Parallel and Distributed Systems* **31**(12), 2802–2818 (2020)
- [11] Li, H., Li, X., Fan, Q., He, Q., Wang, X., Leung, V.C.: Adaptive model partitioning and pruning for collaborative dnn inference in mobile edge-cloud computing networks. *IEEE Transactions on Mobile Computing* (2025)
- [12] Li, S., Zhao, Y., Varma, R., Salpekar, O., Noordhuis, P., Li, T., Paszke, A., Smith, J., Vaughan, B., Damania, P., et al.: Pytorch distributed: Experiences on accelerating data parallel training. *arXiv preprint arXiv:2006.15704* (2020)

- [13] Ma, Y., Wang, Y., Tang, B.: Joint optimization of model partitioning and resource allocation for multi-exit dnns in edge-device collaboration. *Electronics* **14**(8) (2025). <https://doi.org/10.3390/electronics14081647>, <https://www.mdpi.com/2079-9292/14/8/1647>
- [14] Ojo, M.O., Giordano, S., Procissi, G., Seitanidis, I.N.: A review of low-end, middle-end, and high-end iot devices. *IEEE Access* **6**, 70528–70554 (2018). <https://doi.org/10.1109/ACCESS.2018.2879615>
- [15] Pan, J., McElhannon, J.: Future edge cloud and edge computing for internet of things applications. *IEEE Internet of Things Journal* **5**(1), 439–449 (2018). <https://doi.org/10.1109/JIOT.2017.2767608>
- [16] Sah, D.K., Vahabi, M., Fotouhi, H.: Real-time inference for iiot using distributed low-power edge clusters. In: 2025 IEEE 11th World Forum on Internet of Things (WF-IoT). pp. 1–3 (2025). <https://doi.org/10.1109/WF-IoT64238.2025.11270629>
- [17] Shen, W., Lin, W., Wu, W., Wu, H., Li, K.: Reinforcement learning-based task scheduling for heterogeneous computing in end-edge-cloud environment. *Cluster Computing* **28**(3), 179 (2025)
- [18] Shinde, P.P., Shah, S.: A review of machine learning and deep learning applications. In: 2018 Fourth International Conference on Computing Communication Control and Automation (ICCUBEA). pp. 1–6 (2018). <https://doi.org/10.1109/ICCUBEA.2018.8697857>
- [19] Ye, P., Lapkovskis, A., Saleh, A., Zhang, Q., Donta, P.K.: Nesy-edge: Neuro-symbolic trustworthy self-healing in the computing continuum. arXiv preprint arXiv:2603.21145 (2026)
- [20] Yu, W., Liang, F., He, X., Hatcher, W.G., Lu, C., Lin, J., Yang, X.: A survey on the edge computing for the internet of things. *IEEE Access* **6**, 6900–6919 (2018). <https://doi.org/10.1109/ACCESS.2017.2778504>
- [21] Zhang, Y., Zhang, Z., Zhao, H.: Adaptive dnn partitioning for edge-cloud systems with meta-reinforcement learning. In: Proceedings of the 18th IEEE/ACM International Conference on Utility and Cloud Computing, UCC '25, Association for Computing Machinery, New York, NY, USA (2026). <https://doi.org/10.1145/3773274.3774271>, <https://doi-org.ezp.sub.su.se/10.1145/3773274.3774271>
- [22] Zhang, Z., Kouzani, A.Z.: Implementation of dnns on iot devices. *Neural Computing and Applications* **32**(5), 1327–1356 (2020)
- [23] Zhao, S., Yao, D., Wan, Y., Wu, G., Jin, H.: Adapcp: Collaborative inference with adaptive cnn partition on distributed edge servers. *ACM Transactions on Autonomous and Adaptive Systems* **20**(4), 1–28 (2025)
- [24] Zhao, Z., Barijough, K.M., Gerstlauer, A.: Deepthings: Distributed adaptive deep learning inference on resource-constrained iot edge clusters. *IEEE Transactions on Computer-Aided Design of Integrated Circuits and Systems* **37**(11), 2348–2359 (2018)